

DEVELOPMENT OF A TUNGSTEN HEAVY ALLOY, W-Ni-Mn, USED AS KINETIC ENERGY PENETRATOR

S. M. Zahraee, M. T. Salehi, H. Arabi and M. Tamizifar

smzahraee@irost.org

Department of Metallurgy and Materials Engineering, Iran University of Science and Technology, Tehran, Iran.

Abstract: The objective of this research was to develop a tungsten heavy alloy (WHA) having a microstructure and properties good enough to penetrate hard rolled steels as deep as possible. In addition this alloy should not have environmental problems as depleted uranium (DU) materials. For this purpose a wide spread literature survey was performed and on the base of information obtained in this survey, three compositions of WHA were chosen for investigation in this research. The alloys namely 90W-7Ni-3Fe, 90W-9Ni-Mn and 90W-8Ni-2Mn were selected and after producing these alloys through powder metallurgy technique, their thermal conductivity, compression flow properties and microstructures were studied. The results of these investigations indicated that W-Ni-Mn alloys had better flow properties and lower thermal conductivities relative to W-Ni-Fe alloy. In addition Mn helped to obtain a finer microstructure in WHA. Worth mentioning that a finer microstructure as well as lower thermal conductivity in this type of alloys increased the penetration depth due to formation of adiabatic shear bands (ASB) during impact.

Keywords: Tungsten heavy alloy, Depleted Uranium (DU), W- Ni-Fe, W- Ni- Mn, Adiabatic Shear Band (ASB), Kinetic Energy Penetrator (KEP).

1. INTRODUCTION

Tungsten heavy alloys are two phase composites materials containing over 80wt% tungsten and normally a balance of nickel/copper, nickel/iron or nickel/iron/cobalt as a ductile matrix. They are prepared by liquid phase sintering (LPS) of blended elemental powders [1]. In view of their unique combination of high strength, density, ductility, low thermal expansion, good machinability and corrosion resistance, WHAs have been used in a variety of areas ranging from radiation shield, counter balances to kinetic energy penetrator [2, 3]. It has been reported [4-6] that other high density materials such as DU are being used as KEP in some region of the world. Although depleted uranium penetrator can effectively penetrate into armors due to their self sharpening properties[7] , but because of their dangerous environmental side effect, use of these types of penetrators are under increasing criticism world wide [8, 9]. It is believed that the self sharpening ability stems from formation of adiabatic shear band within a material as it impact an object. The details of influencing factors on formation of ASB are discussed

elsewhere [3, 10-11]. Among the factors affecting the formation of ASB, thermal conductivity and tungsten grain size, have the most important role[12, 13]. This is said to be due to the adiabatic condition which is directly related to thermal conduction of the material and smaller tungsten grain size that favor the propagation of the shear bands. The thermal conductivity of Mn is very low (7.8w/mk) i.e. one tenth of thermal conductivity of Fe (78.2W/mk). Therefore it seems addition of Mn instead of Fe to the conventional heavy alloy system can promote formation of ASBs. Since no published phase diagram is available for W-Ni-Mn system, it is not possible to predict exactly the amount of tungsten that would be taken in solution during LPS of W-Ni-Mn alloy. However the amount of tungsten that can be taken into solution within the Ni-Mn matrix during LPS of W-Ni-Mn alloy has been reported to be very limited [13, 14]. The growth of W-grains by Ostwald-ripening mechanism within Ni-Mn matrix can not be substantial due to very limited solution of W within the matrix; hence one can expect to observe smaller W-grains in Ni-Mn alloys.

The objective of this research was to investigate the effect of Mn addition instead of Fe to a W-Ni alloy in order to monitor the microstructure changes as well as thermal conductivity variation, flow properties and finally to compare these properties with those of W-Ni-Fe alloys.

2. EXPERIMENTAL PROCEDURES

2.1. Sample Preparation

Powders of pure tungsten, nickel, iron and manganese were used to produce the alloys. Mean particle size of tungsten powder was $5\mu\text{m}$ while Ni, Fe and Mn powders had mean particle size of less than $5\mu\text{m}$. Each powder was weighed to get the proper composition of 90W-7Ni-3Fe, 90W-9Ni-Mn and 90W-8Ni-2Mn alloys. To obtain a good homogenous blend of each composition a turbula mixer for a period of 45 minutes was used. Then the mixed powders were compacted by cold isostatic press at 200 MPa. Finally the green compacts of the above mentioned alloys sintered in hydrogen atmosphere at 1550°C , 1500°C and 1400°C respectively, for 60 minutes. The sintered density obtained for each alloy was above 99.6% of its theoretical density. After sintering, a post-sintering heat treatment at 1250°C for a period of 120 minutes under vacuum (5×10^{-2} mbar) was applied to remove hydrogen and eliminate hydrogen embrittlement of the samples.

2.2. Characterization

Compression test specimens with a height of 12 and diameter of 8 mm were machined from the sintered bars according to ASTM E8. Three compression tests for each composition were carried out at a cross-head speed of 0.5mm/min using an Instron machine 1496-2D. For the thermal conductivity measurement 2 samples from each composition having a diameter of 40 and a height of 10mm were prepared and the test conducted according to ASTM E1225, with UnithermTM3141 measuring system. To investigate the microstructure of the alloys, the specimens were bisected perpendicular to the longitudinal direction of the sample by a diamond saw. The longitudinal sections were then mounted and metallographically prepared for micro structural study. The prepared sample were deeped in Muorakami's etchant for a period of 30 seconds before being subjected to

micro structural studies by scanning electron microscopy (SEM). An Image analyzer (IA) was used for determining tungsten grains size of the samples.

3. RESULTS AND DISCUSSION

3.1. Mechanical Properties

The compression flow curves of the different samples are presented in Fig. 1.

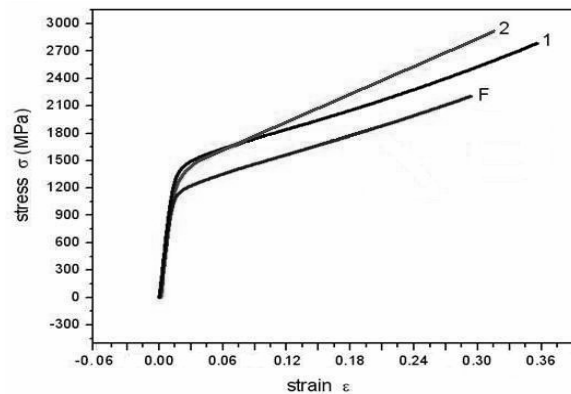


Fig. 1. Compression flow curve of (F) 90W-7Ni-3Fe, (1) 90W-9Ni-Mn (2) 90W-8Ni-2Mn.

The flow curves presented in this figure indicate that the flow properties as well as the resilience and toughness moduli of W-Ni-Mn samples were improved compared with those of W-Ni-Fe. One may seek the cause of these improvements in mechanical properties in the microstructures of W-Ni-Mn alloys developed during processing. Since low solubility of tungsten in alloying element is favorable to slow grain growth and allow microstructural refinement which consequently yields high mechanical performance and the tungsten solubility in the Ni-Mn matrix is very low [13,14] then one expects that by increasing Mn content in W-Ni matrix, the W-grains become smaller than these grains in W-Ni-Fe alloys. Smaller grains mean more grain boundaries which result to an increase in the strength of material at low temperatures. Fig. 2 shows the effect of addition of Mn in reducing W-grains size in comparison to W-grains size of W-Ni-Fe system as show in Fig. 3.

3.2. Thermal Conductivity

The thermal conductivity of 90W-7Ni-3Fe, 90W-9Ni-Mn and 90W-8Ni-2Mn was 70, 51 and 45 W/m-k respectively. The thermal conductivity of Mn is much lower than that of Fe.

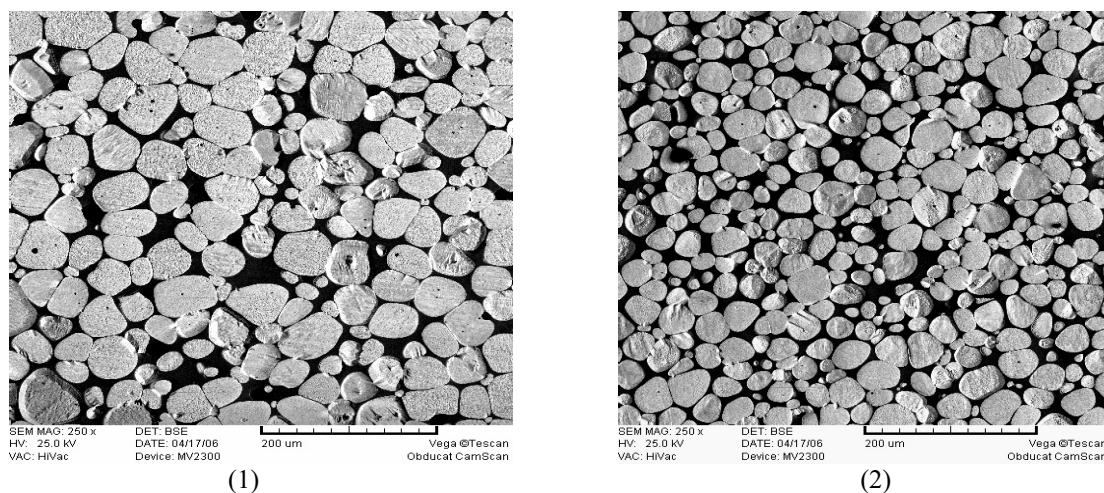


Fig. 2. Microstructure of (1) 90W-9Ni-Mn (2) 90W-8Ni-2Mn alloys.

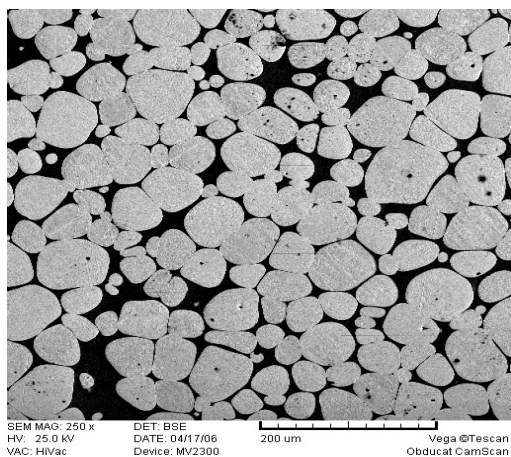


Fig. 3. Microstructure of 90W-7Ni-3Fe alloy.

Therefore addition of Mn to the composition of WHA expected to lower its thermal conductivity much more than that of Fe. The reported thermal conductivity of 90W-7Ni-3Fe alloy by Beijing Advanced Materials co. Ltd. (BAM) is 75W/m-k which is approximately consistent with the thermal conductivity of this type of alloy measured in this research. The small differences observed in the measured thermal conductivity of W-Ni-Fe sample with the reported thermal conductivity of this alloy might be due to the difference in sintering cycle applied in this alloy. Since application of longer sintering time and/or higher sintering temperature cause a higher amount of tungsten, (which has thermal conductivity of 170 W/m-K), to dissolve in Ni-Fe matrix [15]. This in turn can increase thermal conductivity of the alloy. So, since one of the objectives of this research was to reduce thermal conductivity of WHA in order to promote their thermal softening according to Bose [12], we can

claim that this objective was achieved by substituting Mn for Fe in WHAs.

3.3. Microstructure study

Typical microstructure for each sintered samples is presented in Figs. 2 & 3. The micrographs presented in these figures show that mean tungsten grain size within Ni-Mn matrix is much smaller than the mean tungsten grain size within Ni-Fe matrix. The average W-grain sizes for 90W-7Ni-3Fe, 90W-9Ni-Mn and 90W-8Ni-2Mn samples were 50, 35 and 27 μ m respectively. Considering the sintering temperature for each sample was selected about 100°C above its liquids temperature in Ni-Fe and Ni-Mn binary diagrams, and the sintering time was the same for all of the samples, one may assume that the sintering cycles applied for the three samples were similar, so under this condition the differences observed in the mean grain sizes of W-grains related to the presence of element Fe or Mn in the composition of the alloy rather than the applied sintered temperature. In other words, the samples having Mn in their composition had smaller W-grain size relative to the sample having Fe and among the specimens with Mn; the one with higher Mn content had smaller W-grains. This indicates that addition of Mn to W-Ni alloys can refine tungsten grain size within W-Ni-Mn matrix. Since another objective of this research was to obtain finer W-grain size within the microstructure, we can claim that this objective was also achieved. Worth mentioning that according to Bose [12] the finer the microstructure of this type of alloy, the easier would be the formation of ASB during high

strain rate impact. Formation mechanism of these bands will be presented in another article in near future.

3.4. Tungsten Solubility in Ni-Mn

Since neither W-Ni-Mn ternary phase diagram nor W-Mn binary phase diagram were available, it was not possible to predict exactly the amount of tungsten that would be taken in solution during LPS of W-Ni-Mn alloy. However, as shown in Fig. 2(1, 2), the mean W-grain sizes decreased as the manganese content increased. This was expected since tungsten has no

solubility in manganese therefore, its solubility in the Ni-Mn matrix should decrease by increasing it's Mn content. This result was confirmed by the EDS profiles obtained from the matrix having different amount of Mn, Fig. 4(a-c).

These spectrographs show by increasing the amount of Mn of the alloys composition, the amount of tungsten solubility decreased. More details concerning the later have been discussed in a separate article which is to be published [16].

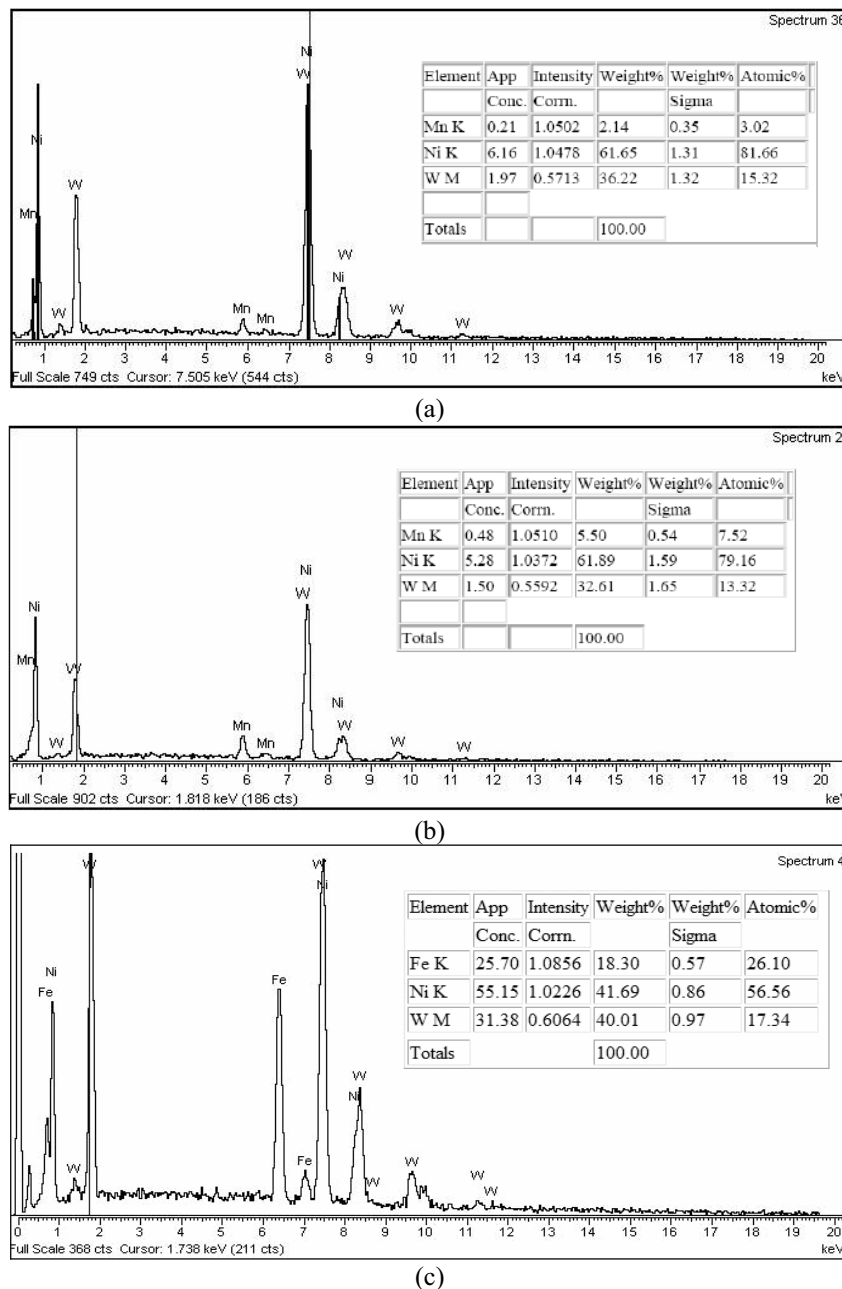


Fig. 4. Typical EDS profiles of the samples matrix (a) 90W-9Ni-1Mn (b) 90W-8Ni-2Mn (c) 90W-7Ni-3Fe

4. CONCLUSIONS

This research showed that:

1. Flow properties of W-Ni-Mn alloys were superior to those of W-Ni-Fe.
2. Higher amount of Mn in 90W-Ni alloy resulted to high strength but slightly lower fracture elongation.
3. Substituting of Fe by Mn in WHAs caused a decrease in the thermal conductivity of the alloy.
4. W-Ni-Mn alloys have finer W-grains than W-Ni-Fe alloy when they develop under similar condition.
5. Higher amount of Mn in 90W-10(Ni-Mn) alloy resulted to smaller W-grain sizes.

ACKNOWLEDGMENT

The authors would like to thank the Khorasan Metallurgy Industry for their support of this research.

REFERENCES

1. German, R. M.; "Liquid Phase Sintering", Plenum Press, New York, 1985.
2. Yadav, s. & Ramesh, K. T.; "the mechanical properties of tungsten based composites at very high strain rates", *Mat. Sci. &Eng. A203*, 1995, 140-153
3. Upadhyaya, A.; "processing strategy for consolidating tungsten heavy alloys for ordnance applications", *Mat. chem. & Phy.* 67, 2001, 101-110
4. Bleise, A. et al; "Properties, use and health effects of depleted uranium (DU): a general over view", *JR. of Env. Rad.* 64, 2003, 93-112.
5. Pöllänen, R. et al.; "characterization of projectiles composed of depleted uranium", *Jr. of Env. Rad.* 64, 2003, 133-142.
6. Giannardi, C. & Dominici, D.; "Military use of depleted uranium: assessment of Prolonged population exposure", *Jr. of Env. Rad.* 64, 2003, 227-236.
7. German, R. M. et al.; "Tungsten heavy alloy rivals depleted Uranium", *Met. Powder, Rep.* Vol. 47, No. 11, 1992, 42-46.
8. Mc clain, D. E. et al.; "Biological effects of embedded depleted uranium (DU): Summary of Armed forces Radio biology Research Institute research, *The Sci. of the total Env.* 274, 2001, 115-118.
9. McLavghlin, J. P. et al.; "Actinide analysis of a depleted uranium penetrator from a 1999 target site in southern Serbia" *Jr. of Env. Rad.* 64, 2003, 155-165.
10. Kim, D. K. et al.; "micro structural study of adiabatic shear bands formed by high speed impact in a tungsten heavy alloy penetrator", *Mat. Sc. & Eng. A249*. 1998, 197-205.
11. Nabil Bassim, M.; "study of the formation of adiabatic shear bands in steel, *Jr. of Mat. Proc. Tech.* 119, 2001, 234-236.
12. Bose, A. et al.; "Influence of microstructure on shear localization in tungsten heavy alloys", *Proc. of 1st Int. Conf. on tungsten & tungsten alloys*, A. Bose, R. J. Dowding (Ed), MPIF, New Jersey, 1992, 291-298.
13. Bose, A.; et al "Development of a new W-Ni-Mn heavy alloy", *Ad. In P/M.*, Vol. 6, Aerospace Refractory & advanced materials, 1991, 425-437
14. Bose, A. "Heavy alloy based on tungsten – Nickel- Manganese", U.S. patent No. 5603073, Feb, 1997
15. German, R. M. et al.; "Sintering time and atmosphere influences on the microstructure and mechanical properties of tungsten heavy alloys", *Met. Trans. A*, Vol.23A, 1992, 211-219
16. Zahraee, S. M. et al.; "Effect of Mn/Ni ratio variation on microstructure of W-Ni-Mn alloy", *Powder Metallurgy Jr.* to be published